

## Band structure of indium oxide: Indirect versus direct band gap

Paul Erhart,<sup>1,\*</sup> Andreas Klein,<sup>1</sup> Russell G. Egdell,<sup>2</sup> and Karsten Albe<sup>1</sup>

<sup>1</sup>*Institut für Materialwissenschaft, Technische Universität Darmstadt, D-64287 Darmstadt, Germany*

<sup>2</sup>*Inorganic Chemistry Laboratory, Oxford University, South Park Road, Oxford OX1 3QR, United Kingdom*

(Received 27 November 2006; published 25 April 2007)

The nature of the band gap of indium oxide is still a matter of debate. Based on optical measurements the presence of an indirect band gap has been suggested, which is 0.9 to 1.1 eV smaller than the direct band gap at the  $\Gamma$  point. This could be caused by strong mixing of O  $2p$  and In  $4d$  orbitals off  $\Gamma$ . We have performed extensive density functional theory calculations using the LDA+ $U$  and the GGA+ $U$  methods to elucidate the contribution of the In  $4d$  states and the effect of spin-orbit coupling on the valence band structure. Although an indirect band gap is obtained, the energy difference between the overall valence band maximum and the highest occupied level at the  $\Gamma$  point is less than 50 meV. It is concluded that the experimental observation cannot be related to the electronic structure of the defect free bulk material.

DOI: [10.1103/PhysRevB.75.153205](https://doi.org/10.1103/PhysRevB.75.153205)

PACS number(s): 71.15.Mb, 71.70.Ej, 71.20.Nr

Indium oxide ( $\text{In}_2\text{O}_3$ ) and tin-doped indium oxide (ITO) are applied, e.g., as solid state gas sensor materials and oxidation catalysts.<sup>1</sup> ITO is mainly used as a transparent electrode material in flat-panel displays and solar cells particularly involving organic materials.<sup>2</sup> In spite of the technological importance of these materials and a variety of both experimental and theoretical studies their band structures are, however, still not fully understood.

In optoelectronic applications the electronic properties of the interfaces are crucial, which can be directly accessed using photoelectron spectroscopy.<sup>3,4</sup> Based on such studies it has been suggested that the surface of  $\text{In}_2\text{O}_3$  and ITO shows a depletion layer,<sup>5-7</sup> which has considerable consequences for the electronic properties of the interfaces.<sup>3,4</sup> The conclusion for a depletion layer is based on the observation of the Fermi level position at the surface, which varies between 2.2 and 3.5 eV with respect to the valence band maximum (VBM).<sup>5-7</sup> This is smaller than the assumed fundamental gap of about 3.6 eV which corresponds to the widely accepted lowest direct gap.<sup>8,9</sup> In contrast, also a considerably smaller indirect gap has been reported by a number of groups,<sup>9,10</sup> which would be consistent with a depletion layer-free flat-band situation at the surface. Since the conduction band minimum is located at the  $\Gamma$  point,<sup>9,11</sup> the indirect band gap must correspond to an off- $\Gamma$  VBM, which might arise from a mixing of O  $2p$  and In  $4d$  states away from the zone center.<sup>12</sup> The presence of an indirect band gap has been questioned due to considerable inconsistency of the available data concerning the magnitude of the indirect gap (2.1–2.7 eV) and the  $k$ -space location of the VBM.<sup>4,7</sup> Instead, surface and grain boundary effects have been invoked to explain the observed optical absorption below the smallest direct gap.

Several theoretical studies have been performed to elucidate the situation for the undoped material: Albanesi *et al.* used a tight-binding method to calculate the band structure of  $\text{In}_2\text{O}_3$  but did not include the In  $4d$  orbitals in the valence.<sup>13</sup> Tanaka and co-workers performed cluster calculations using the discrete-variational  $X\alpha$  method and a linear combination of atomic orbitals including the In  $4d$  electrons in the valence.<sup>14</sup> They located the In  $4d$  band between 10 and 12 eV below the VBM and observed an antibonding contri-

bution near the top of the valence band due to hybridization between In  $4d$  and O  $2p$  states. Odaka *et al.* carried out density functional theory (DFT) calculations using the linear muffin-tin orbital method in combination with the atomic sphere approximation.<sup>15</sup> They observed an indirect band gap with the VBM at the  $H$  point and observed a negative curvature of the valence band near the  $\Gamma$  point. The energy difference between the highest occupied levels at  $H$  and  $\Gamma$  was, however, less than 0.1 eV, which is significantly smaller than the difference between the experimentally suggested direct and indirect band gaps (0.87–1.13 eV). While these calculations suffered from an underestimation of the band gap typical for DFT, Mi and coworkers adopted a scissor operator to correct for this shortcoming.<sup>16</sup> However, they did not include the In  $4d$  electrons in the valence. The most elaborate calculations up to date were carried out by Mryasov and Freeman who used a full potential linear muffin-tin orbital approach and reported a direct band gap of 1.0 eV.<sup>17</sup>

In summary, the studies published so far neither provide clear evidence for the presence of an indirect band gap, nor rule out its existence. In the present work, we present calculations that provide strong evidence that the large difference between the “indirect” and direct band gaps determined experimentally is not due to the bulk electronic structure. To this end, we pay particular attention to two aspects which, in principle, have the potential to change markedly the outcome of the calculations, but were not considered in previous works. (1) In many transition metal oxides including—as will be shown below— $\text{In}_2\text{O}_3$  the description of the metal  $d$  levels using the local density or generalized gradient approximation is flawed.<sup>18,19</sup> The energetic position of the In  $4d$ -derived orbitals, however, affects the hybridization of In  $4d$  levels with O  $2s$  and O  $2p$  levels, which also has an impact on the structure near the VBM. (2) In other In compounds the In  $4d$  levels are known to split due to spin-orbit coupling by as much as 0.86 eV.<sup>20</sup> If a splitting of this magnitude occurred near the top of the valence band an indirect band gap could result.

In the following, we show that correcting the position of the In  $4d$  orbitals leads to a significantly better agreement between data from photoelectron spectroscopic measure-

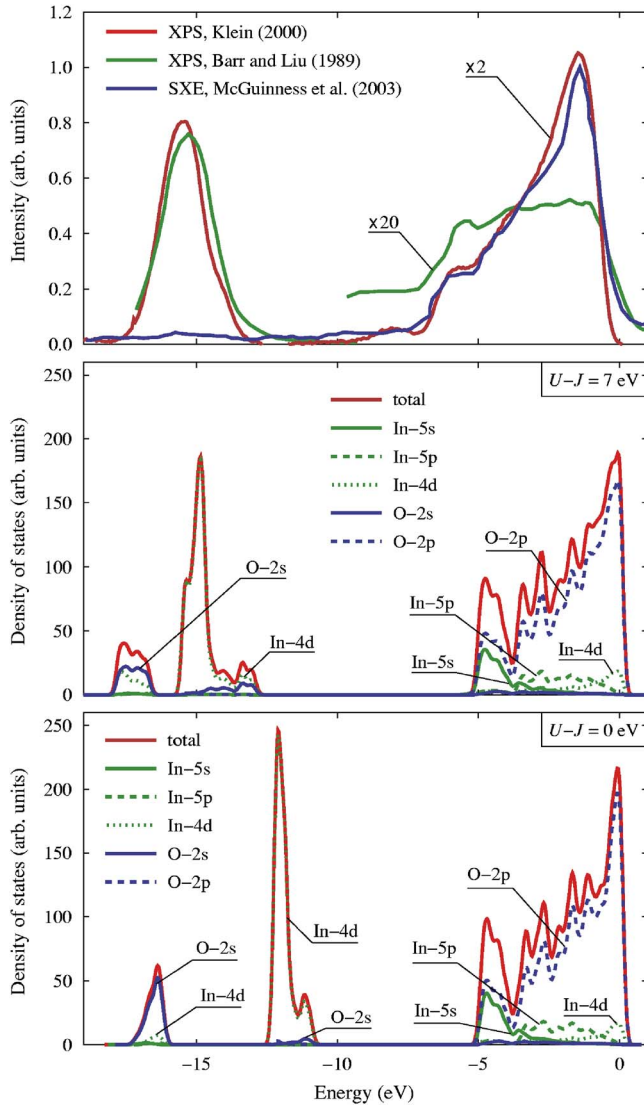


FIG. 1. (Color online) Total and partial DOSs from GGA+ $U$  calculations using  $\bar{U}-\bar{J}=0$  and 7 eV. The results of x-ray photoelectron spectroscopy (XPS, Refs. 5 and 28) and soft x-ray emission (SXE, Ref. 12) spectroscopy measurements are shown for comparison. For better visualization the calculated density of states was broadened using a Gaussian filter with 0.1 eV and multiplied by a factor of 5 for energies larger than  $-8$  eV.

ments and the calculated density of states (DOS). In addition, while the In  $4d$ -O  $2p$  mixing is reduced, the In  $4d$ -O  $2s$  hybridization increases. Finally, it is demonstrated that the inclusion of spin-orbit coupling, causes a splitting of the deep In  $4d$  band, but does not affect levels near the VBM. Note that the effects described above pertain to the valence band only. A description within DFT is therefore reliable and the band gap underestimation and the shortcomings with respect to the description of excited states intrinsic to DFT are not of concern.

Density functional theory calculations were carried out employing the Vienna *ab initio* simulation package (VASP).<sup>22</sup> The ionic cores were represented using the projector-augmented wave method<sup>23</sup> including the In  $4d$  electrons in the valence. Both the local density approximation<sup>24</sup> (LDA)

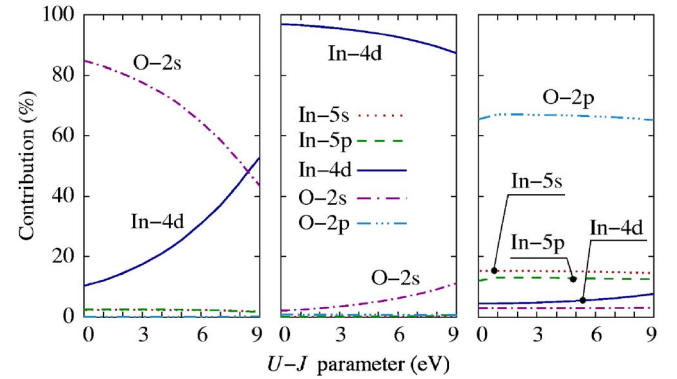


FIG. 2. (Color online) Contribution of different atomic orbitals to the three main bands of the valence band density of states (GGA+ $U$ ). The left panel shows the O  $2s$ -dominated band positioned at the largest binding energies, the middle panel the In  $4d$ -dominated, and the right panel the O  $2p$ -dominated band.

and the generalized gradient approximation (GGA) in the Perdew-Burke-Ernzerhof parametrization<sup>25</sup> were employed. If the “standard” LDA or GGA functionals are used the binding energy of the rather localized In  $4d$  levels is underestimated due to shortcomings intrinsic in the construction of these functionals. In the present work, this was taken into account by using the semiempirical LDA+ $U$  and GGA+ $U$  schemes<sup>19</sup> in the version by Dudarev *et al.*<sup>26</sup> which incorporates self-interaction corrections into the LDA and GGA functionals. The self-interaction parameter  $\bar{U}-\bar{J}$  was varied between 0 (no correction) and 9 eV. Brillouin zone sampling was performed using a  $3 \times 3 \times 3$   $k$ -point grid and the plane wave energy cutoff was set to 500 eV providing a convergence of the total energy better than 1 meV/fu. For each setup the energy-volume curve was evaluated allowing for full relaxation at each volume and the data were fitted to the Birch-Murnaghan equation of state.<sup>27</sup> The band structure as well as the site and momentum-projected DOS were subsequently calculated at the theoretical equilibrium lattice constant. In order to assess the effect of spin-orbit coupling, additional calculations were carried out for  $\bar{U}-\bar{J}=0$  and 7 eV. Using the configurations from the non-spin-polarized calculations, the charge density was determined self-consistently allowing for noncollinear spin configurations without symmetry constraints (and without ionic relaxation). The resultant density was subsequently employed for calculating the full band structure.

We first focus on the role of the In  $4d$  electrons. If the uncorrected GGA (or equivalently LDA) functional is used ( $\bar{U}-\bar{J}=0$  eV), the In  $4d$  band in the DOS is located at significantly lower binding energies than in experiments (Fig. 1). Increasing the  $\bar{U}-\bar{J}$  parameter most prominently affects the position of the deep In  $4d$ -dominated band which is shifted to more negative binding energies. The GGA+ $U$  (LDA+ $U$ ) method allows us to correct this shortcoming as demonstrated in the middle panel of Fig. 1. As a result, the hybridization and thus the mixing of the different orbitals is affected. This leads to marked changes in the partial DOS (Fig. 1). The effect is also illustrated in Fig. 2 which shows

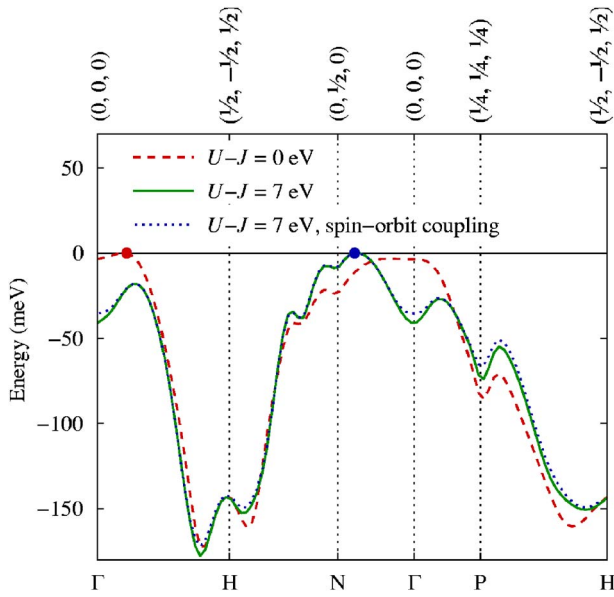


FIG. 3. (Color online) Impact of position of In 4d states and spin-orbit coupling on the position of the valence band maximum in reciprocal space.

how the relative contributions of In- and O-derived orbitals to the three main bands (O 2s, In 4d, and O 2p dominated) in the valence band DOS vary as a function of the  $\bar{U}-\bar{J}$  parameter. Here, the relative contributions have been determined as the integral over the partial densities of states (site and orbital projected) divided by the total DOS. The three main bands are defined by the minima in the total DOS. The most notable changes are observed in the lowest band which is dominated by O 2s states. As the In 4d levels are pushed downward (reproducing the experimental situation) the mixing of O 2s with In 4d strongly increases. A similar effect—though much weaker—also occurs for the uppermost part of the valence band where the O 2p–In 4d mixing is enhanced. (The hybridization of cation *d* orbitals with anion *s* orbitals has also been described in other binary semiconductors<sup>29</sup>).

While the correction of the In 4d orbitals leads to a different mixing between In 4d – and oxygen-derived states, the band structure near the VBM is weakly affected (Fig. 3). The

TABLE I. Calculated properties of In<sub>2</sub>O<sub>3</sub> in comparison with experiment (Ref. 21).  $E_c$ , cohesive energy (eV/f.u.);  $a_0$ , lattice constant (Å);  $V_0$ , equilibrium volume (Å<sup>3</sup>);  $B, B'$ , bulk modulus (GPa) and its pressure derivative;  $x_{\text{In } d}, x_{\text{O}}, y_{\text{O}}, z_{\text{O}}$ , Wyckoff positions;  $E_G^\Gamma$ , band gap at  $\Gamma$  point (eV);  $E_G^{\text{ind}}$ , indirect band gap (eV);  $\Delta E_{\text{SO}}$ , splitting of In 4d peak due to spin-orbit (SO) coupling (eV).

	Expt.	LDA				GGA,PBE	
		$\bar{U}-\bar{J}$					
		0.0	7.0	0.0	7.0		
$E_c$		-31.91	-33.32	-28.27	-29.29		
$a_0$	10.121	10.077	9.783	10.306	10.027		
$V_0$	64.80	63.96	58.52	68.41	63.01		
$B$		168	180	141	149		
$B'$		4.8	4.6	4.6	4.6		
$x_{\text{In } d}$	0.466	0.467	0.465	0.466	0.466		
$x_{\text{O}}$	0.390	0.390	0.390	0.390	0.390		
$y_{\text{O}}$	0.155	0.154	0.156	0.154	0.155		
$z_{\text{O}}$	0.382	0.382	0.383	0.382	0.383		
$E_G^\Gamma$	3.56–3.75	1.21	2.21	0.93	1.83		
$E_G^{\text{ind}}$	2.62–2.69	1.20	2.18	0.93	1.79		
$E_G^\Gamma$ (with SO)		1.16	2.20		1.82		
$E_G^{\text{ind}}$ (with SO)		1.16	2.18		1.81		
$\Delta E_{\text{SO}}$	(0.86 <sup>a</sup> )	0.86	0.90	0.85	0.89		

<sup>a</sup>Experimental observation in other In compounds (Ref. 20).

location of the VBM depends sensitively on the details of the calculation. The energy difference from the  $\Gamma$  point is, however, always less than 50 meV and thus much too small to explain the large difference between the direct and indirect band gaps inferred from experiments.<sup>9,10</sup> (Even for a value for  $\bar{U}-\bar{J}$  as large as 9 eV, which strongly overestimates the binding energy for the In 4d levels, the energy difference is at most 65 meV). Along with the lowering of the In 4d bands, the repulsion between these states and the conduction band increases, which leads to an enlargement of the band gap (Table I). Figure 4 also reveals a broadening of the In 4d band due to an increasing contribution of O 2s states.

In order to rule out that spin-orbit coupling can lead to a

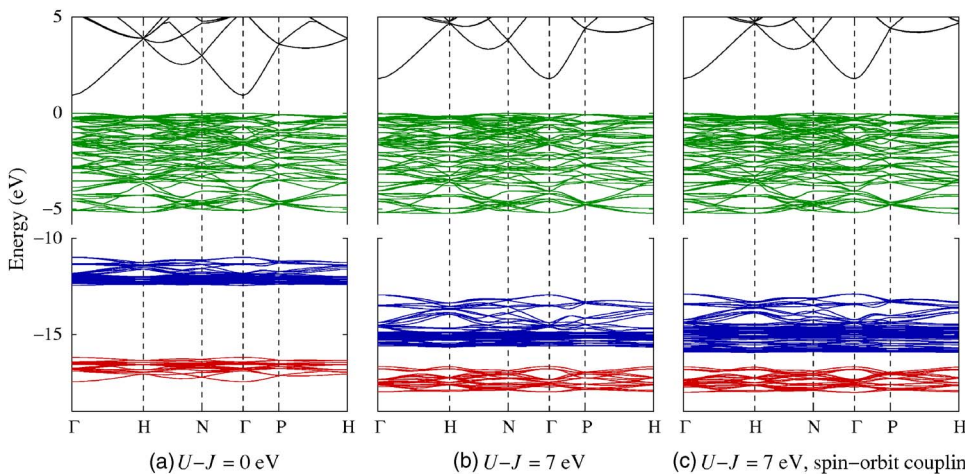


FIG. 4. (Color online) Band structures for In<sub>2</sub>O<sub>3</sub> from GGA +*U* calculations using  $\bar{U}-\bar{J}=0$  and 7 eV, and including spin-orbit coupling.

level splitting sufficiently large to give rise to a pronounced indirect band gap, additional noncollinear spin-polarized calculations were carried out. The resulting band structure and the effect on the most upper part of the valence band are shown in Figs. 3 and 4. It is found that spin-orbit coupling leads to splitting of the lower In  $4d$  band. Depending on the exchange-correlation functional and the  $\bar{U}-\bar{J}$  parameter, the two maxima in the DOS are separated by 0.85–0.90 eV (Table I). These values are in excellent agreement with experimental data for other In compounds.<sup>20</sup> The other bands of the DOS as well as the band structure are, however, hardly affected. In particular, the small contribution of In  $4d$  orbitals to the DOS near the top of the valence band (Fig. 1) as well as the structure of the VBM in  $k$  space (Fig. 3) remain unaffected.

In summary, density functional theory calculations were carried out in order to elucidate the structure of the valence band of indium oxide and to resolve the character of the band

gap. To this end, the role of the In  $4d$  electrons and the effect of spin-orbit coupling were considered. Correcting the In  $4d$  orbitals enhances the hybridization of In  $4d$  with both O  $2s$  and—to a significantly weaker extent—O  $2p$  states. Simultaneously, the position of the valence band maximum is shifted slightly off  $\Gamma$  but the difference between the VBM at the  $\Gamma$  point and the overall VBM never exceeds 50 meV. The inclusion of spin-orbit coupling leads to a yet smaller change of the structure of the valence band. The present calculations provide strong support that the experimental observations, which have been interpreted as evidence for a pronounced indirect band gap, cannot be related to the electronic structure of the defect free bulk.

This project was funded by the Sonderforschungsbereich 595 “Fatigue in functional materials” of the Deutsche Forschungsgemeinschaft. Discussions with Y. Gassenbauer are gratefully acknowledged.

\*Electronic address: paul.erhart@web.de

- <sup>1</sup>E. Gagaoudakis *et al.*, Sens. Actuators B **80**, 155 (2001); N. G. Patel, P. D. Patel, and V. S. Vaishnav, *ibid.* **96**, 180 (2003); V. Golovanov *et al.*, *ibid.* **106**, 563 (2005); A. Gurlo *et al.*, *ibid.* **15**, 4377 (2003).
- <sup>2</sup>L. S. Hung and C. H. Chen, Mater. Sci. Eng., R. **39**, 143 (2002); C. J. Brabec, N. S. Sariciftci, and J. C. Hummelen, Adv. Funct. Mater. **11**, 15 (2001); P. Peumans, A. Yakimov, and S. R. Forrest, J. Appl. Phys. **93**, 3693 (2003).
- <sup>3</sup>O. Lang *et al.*, J. Appl. Phys. **86**, 5687 (1999); J. Fritsche *et al.*, Thin Solid Films **403-404**, 252 (2002); F. Rüggeberg and A. Klein, Appl. Phys. A: Mater. Sci. Process. **82**, 281 (2006).
- <sup>4</sup>Y. Gassenbauer and A. Klein, J. Phys. Chem. B **110**, 4793 (2006).
- <sup>5</sup>A. Klein, Appl. Phys. Lett. **77**, 2009 (2000).
- <sup>6</sup>Y. Gassenbauer *et al.*, Phys. Rev. B **73**, 245312 (2006).
- <sup>7</sup>S. P. Harvey *et al.*, J. Phys. D **39**, 3959 (2006).
- <sup>8</sup>I. Hamberg and C. G. Granqvist, J. Appl. Phys. **60**, R123 (1986).
- <sup>9</sup>R. L. Weiher and R. P. Ley, J. Appl. Phys. **37**, 299 (1966).
- <sup>10</sup>C. A. Pan and T. P. Ma, Appl. Phys. Lett. **37**, 163 (1980); J. F. McCann and J. O. M. Bockris, J. Electrochem. Soc. **128**, 1719 (1981); F.-T. Liou *et al.*, J. Appl. Electrochem. **13**, 377 (1982); J. Szczyrbowski, A. Dietrich, and H. Hoffmann, Phys. Status Solidi A **78**, 243 (1983); F. Martino *et al.*, Phys. Rev. B **72**, 085437 (2005).
- <sup>11</sup>R. L. Weiher and B. G. Dick, Jr., J. Appl. Phys. **35**, 3511 (1964).
- <sup>12</sup>C. McGuinness *et al.*, Phys. Rev. B **68**, 165104 (2003).
- <sup>13</sup>E. A. Albanesi *et al.*, Solid State Commun. **86**, 27 (1993).
- <sup>14</sup>I. Tanaka, M. Mizuno, and H. Adachi, Phys. Rev. B **56**, 3536 (1997).
- <sup>15</sup>H. Odaka *et al.*, Jpn. J. Appl. Phys., Part 1 **36**, 5551 (1997).
- <sup>16</sup>Y. Mi, H. Odaka, and S. Iwata, Jpn. J. Appl. Phys., Part 1 **38**, 3453 (1999).
- <sup>17</sup>O. N. Mryasov and A. J. Freeman, Phys. Rev. B **64**, 233111 (2001).
- <sup>18</sup>D. Vogel, P. Krüger, and J. Pollmann, Phys. Rev. B **54**, 5495 (1996).
- <sup>19</sup>V. I. Anisimov, J. Zaanen, and O. K. Andersen, Phys. Rev. B **44**, 943 (1991).
- <sup>20</sup>R. A. Pollak *et al.*, Phys. Rev. Lett. **29**, 274 (1972); T. Kendelewicz *et al.*, Phys. Rev. B **36**, 6543 (1987).
- <sup>21</sup>G. B. González *et al.*, J. Appl. Phys. **89**, 2550 (2001); *Handbook of Chemistry and Physics*, 85th ed., edited by D. R. Lide (CRC Press, Boca Raton, FL, 2004).
- <sup>22</sup>G. Kresse and J. Hafner, Phys. Rev. B **47**, 558 (1993); **49**, 14251 (1994); G. Kresse and J. Furthmüller, *ibid.* **54**, 11169 (1996); Comput. Mater. Sci. **6**, 15 (1996).
- <sup>23</sup>P. E. Blöchl, Phys. Rev. B **50**, 17953 (1994); G. Kresse and D. Joubert, *ibid.* **59**, 1758 (1999).
- <sup>24</sup>D. M. Ceperley and B. J. Alder, Phys. Rev. Lett. **45**, 566 (1980).
- <sup>25</sup>J. P. Perdew, K. Burke, and M. Ernzerhof, Phys. Rev. Lett. **77**, 3865 (1996); **78**, 1396(E) (1997).
- <sup>26</sup>S. L. Dudarev *et al.*, Phys. Rev. B **57**, 1505 (1998).
- <sup>27</sup>F. Birch, J. Geophys. Res. **83**, 1257 (1978).
- <sup>28</sup>T. L. Barr and Y. L. Liu, J. Phys. Chem. Solids **50**, 657 (1989).
- <sup>29</sup>C. Persson and A. Zunger, Phys. Rev. B **68**, 073205 (2003).